PHYSICAL REVIEW B VOLUME 18, NUMBER 8 15 OCTOBER 1978

Specific heats and lattice dynamics of cuprous halides

Z. Vardeny,* G. Gilat, and D. Moses†
Department of Physics, Technion—Israel Institute of Technology, Haifa, Israel
(Received 11 February 1977)

The specific heats $C_p(T)$ of CuCl, CuBr, and CuI were measured by the adiabatic calorimetric technique. The corresponding Debye temperature for each crystal is given and a comparison between the results is drawn. The room-temperature phonon dispersion relations for these cystals are fitted by a nine-parameter shell model which gives good fits to CuBr and CuI and a fair fit to CuCl. These model calculations are used to compute $C_v(T)$ for the three cuprous halides and the calculated results are compared with experiment. The agreement is good for the range of $T > 30$°K and less so for $T < 30$°K where discrepancies are to be expected due to anharmonicity that affects the theoretical results. For CuCl we also obtain the Grüneisen parameter $\gamma(T)$ using thermal expansion data.

I. INTRODUCTION

The cuprous halides CuCl, CuBr, and CuI have recently focused a considerable interest despite their simple zinc-blende (ZB) structure. This structure is typical to covalent bonding, but their ionicity,[1] in particular that of CuCl, is among the highest of all ZB crystals. Binary compounds of higher ionicity tend to crystallize in the NaCl or CsCl structures.[2] It is therefore not surprising that their physical behavior is somewhat peculiar and that CuCl is more anomalous than CuBr and CuI.

The physical behavior concerns mainly the structural stability of the cuprous halides, which is rather low. They all exhibit structural phase transitions at a relatively low hydrostatic pressure[3-5] at room temperatures. These are yet not fully characterized but they include an outstanding phase transition of CuCl into a metallic state.[6] Another feature concerns the elastic constants of the Cu halides, particularly the shear and bulk moduli, which are abnormally small.[7] For CuCl, they decrease with increasing pressure.[8] Another peculiarity is the large negative thermal-expansion coefficient[9] of CuCl and CuBr below 100 °K and 50 °K, respectively. This property is related to the negative Grüneisen parameters of the low-energy TA branches.[10,11]

The dynamical properties of the Cu halides as determined by Raman scattering[12-15] and ir absorption[16,17] are of considerable interest because of their unusual properties. In the cases of CuCl[13,14] and CuBr[12] a broad peak related to the TO photons was observed. The interpretation of this anomaly was given[12,15] by the phonon hybridization model of Ruvalds and Zawadowsky.[18] Very recently[19] an inelastic-neutron-scattering experiment at 4.2 °K was performed to study the phonon shapes of CuCl near the Γ points. This experiment is still in progress, but it also shows phonon shape peculiarities.

The lattice dynamics of the Cu halides were investigated by means of inelastic neutron scattering.[20-24] Two common features of the phonon spectra can be sorted out: the TA modes are unusually flat along all high-symmetry directions, and an energy gap appears between the acoustical and the optical branches. A rigid-ion model was used successfully to fit the phonon dispersion curves for[22] CuI and[21] CuBr, but it failed in the case of CuCl.[20] Recently a double-shell model (DSM) was used successfully[24] to fit the phonon dispersion relations of CuCl at 300 °K.

Specific-heat data are essential for the interpretation of the dynamical properties of the crystals. In an earlier paper,[25] we reported the measurements of the specific hear of CuCl. Presently we report the measurements of the specific heats of CuCl, CuBr, and CuI, in the range of 5 to 160 °K.

In Sec. II we describe the experimental details and in Sec. III the analysis of the measurements is brought and comparisons between the three halides are drawn. In Sec. IV the measured phonon spectra[20-22] are fitted to a nine-parameter shell model. The resulting specific-heat calculations are presented in Sec. V and compared with the measured data. In Sec. VI the Grüneisen parameters of the crystals are calculated by using the data of Barron *et al.*[10] and the resulting anharmonic properties are discussed. Sec. VII is devoted to a discussion and conclusion of the article.

II. EXPERIMENT

The specific heat $C_p(T)$ at constant pressure was performed by an adiabatic calorimetric system[28] including an on-line computer. The system

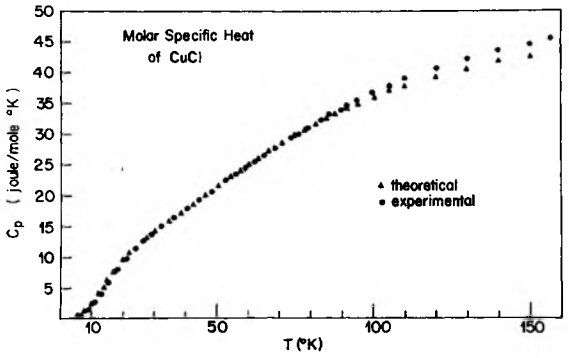

FIG. 1. Theoretical and experimental molar-specific heats of CuCl as functions of temperature.

was mostly operated by a discrete heating mode, and C_p was obtained as a function of T through a computer-stored calibration curve. The computer was programmed to correct the specific-heat results for possible heat leaks during the heating period of the sample. The temperature rises were adjusted to the midpoints of the heating periods from a linear extrapolation of the lines fitted to the temperature points before and after the drift periods. The calculated energy supplied to the sample during the heating and the resulting rise in T give C_p at the average temperature reading.

The thermometers used in the experiments were an Allen-Bradley carbon resistor and a platinum thermometer of a small physical size for the low- and the high-temperature ranges, respectively. The thermometers were calibrated against helium vapor pressure and against calibrated germanium and platinum thermometers.

The samples used for the measurements were installed between two thin copper plates glued to a heater and thermometers. Prior to the actual measurements we determined the heat capacity of the "empty" calorimeter by attaching the copper plates against one another. To test the system, the C_p of a highly-pure copper sample was measured. The results for the copper sample fitted previously published data[29] within deviations of less than 0.3%.

The samples of CuCl and CuBr used in these measurements were single crystals of masses 1.6 and 2.7 g, respectively. For CuI, C_p was measured for a polycrystalline ingot of 4.5 g. The calorimeter heat capacity was in the range of 10–30% of the total heat capacity. The data of C_p in the range of 5 to 160 °K are shown in Figs. 1–3 for the three compounds. The experimental error for C_p at low temperature is about 0.3% and it increases gradually at 2% at 160°K. The reason for this is related to the decrease in the head conductivity as a function of T. The differences between C_p and C_v were found to be small in comparison with experimental uncertainties over all the temperature range and therefore we assume hereafter that within the experimental error $C_p = C_v$.

III. EXPERIMENTAL ANALYSIS

Since C_v varies over several orders of magnitudes in the range 5–160 °K, it is customary to employ the more sensitive characteristic Debye

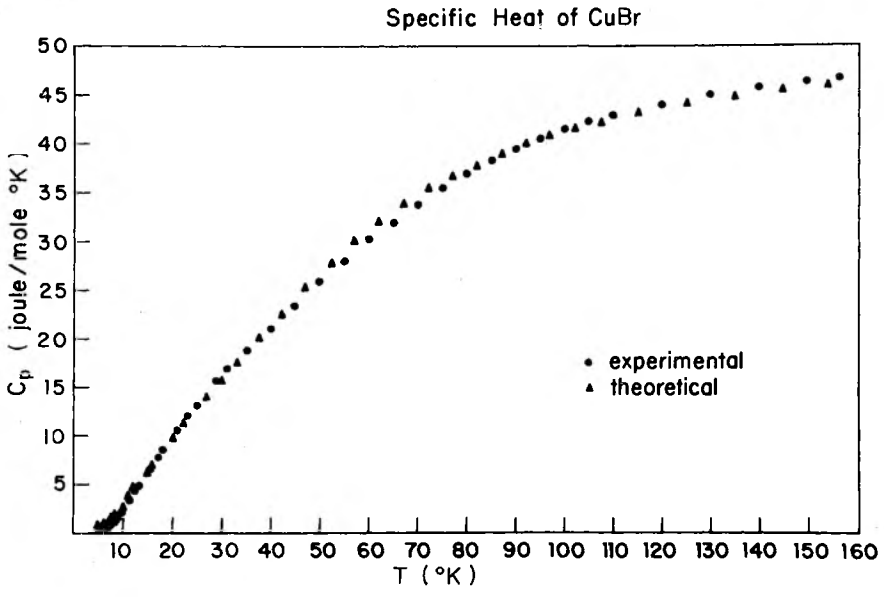

FIG. 2. Theoretical and experimental molar-specific heats of CuBr as functions of temperature.

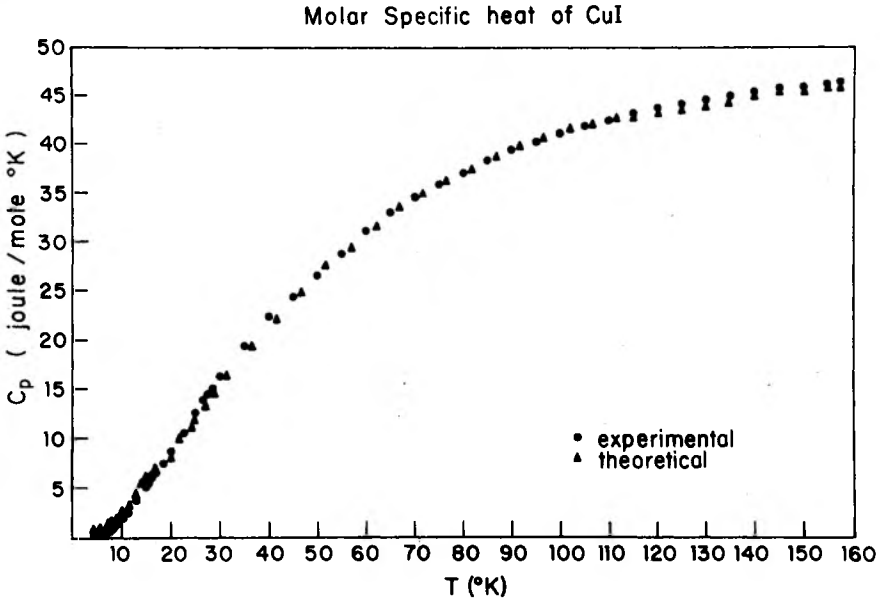

FIG. 3. Theoretical and experimental molar-specific heats of CuI as functions of temperature.

temperature $\Theta_D(T)$, which varies over much a smaller range. The results for the $_D(T)$ for the three Cu halides shown in Figs. 4–6 were calculated from the individual measurements of C_v using tabulated values of the Debye function:

$$C_v(T) = 18Nk_B(T/\Theta_D)^3 \int_0^{\Theta_D/T} \frac{x^4 e^x}{(e^x - 1)^3} dx, \qquad (1)$$

where k_B is the Boltzman factor and N is the Avogadro number. $\Theta_D(0)$ is obtained by extrapolating C_v/T^3 vs T^2 at $T = 0$ °K. Values of $\Theta_D(0)$, $\Theta_D(\infty)$, and other relevant data are given in Table I.

In Table I, we also bring $\Theta_D^{el}(0)$ of CuBr and CuI calculated from the elastic-constants data of the Cu halides which were measured by Hanson[7] *et al.* using de Launay tables.[26] $\Theta_D^{el}(0)$ of CuCl was also calculated by Barron *et al.*[10] who included the piezoelectric effect[8] in CuCl caused by electromechanical contributions to the elastic constants. This effect is absent in C_{44}^E measured along the [100] direction, but it affects C_{44}^D measured along the [110] direction, and $C_{44}^D > C_{44}^E$. Barron[10] *et al.* compared $\Theta_D^{el}(0)$ using either C_{44}^E or C_{44}^D and obtained $\Theta_D^{el}(0) = 178.6°$ and 184.3°, respectively. The weighted average for CuCl is $\Theta_D^{el}(0) = 180.4$ °K closer to the value obtained by using C_{44}^E alone. For this reason we use C_{44}^E alone for CuBr and CuI, where the piezoelectric is considerably smaller[7] than it is for CuCl.

Our measured values of C_p fit excellently with the C_p measured by Barron *et al.* in the range of 5–16 °K. Below 5 °K our extrapolated value for $\Theta_D(0)$ using C_v/T_3 vs T^2 fails to reproduce the considerable increase in Θ_D observed by Barron *et al.* (see Fig. 4).

The curves of $\Theta_D(T)$ for the three Cu halides show all minima of value of about $0.75\Theta_D(0)$ at

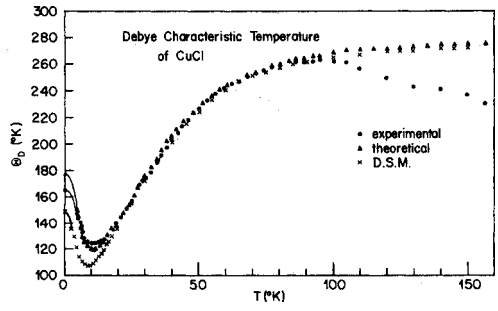

FIG. 4. Experimental and calculated Debye temperature Θ_D of CuCl as a function of temperature. The values of Θ_D below 5 °K are extrapolated. DSM refers to the double shell model in Sec. V.

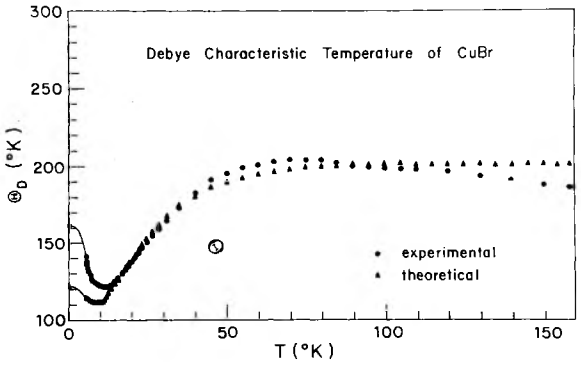

FIG. 5. Experimental and calculated Debye temperature Θ_D of CuBr as a function of temperature. The values of Θ_D below 5 °K are extrapolated.

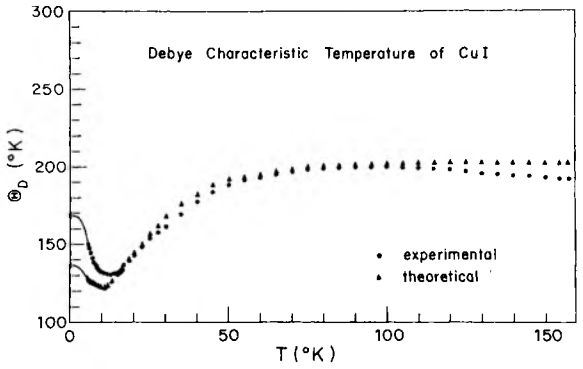

FIG. 6. Experimental and calculated Debye temperature Θ_D of CuI as a function of temperature. The values of Θ_D below 5 °K are extrapolated.

temperatures of about $\frac{1}{14}\Theta_D(0)$. This minima in $\Theta_D(T)$ are regular in most crystals of different structures and natures.

Another common feature of $\Theta_D(T)$ of the cuprous halides is the relative large variation in value over the range 0–100 °K. The rise in $\Theta_D(T)$ beyond its minimum is much larger than usual. We attribute the origin of this growth in $\Theta_D(T)$ to the gap in $g(\nu)$ in the frequency range 1.5–2.5 THz, which is common to the three cuprous halides. This gap is caused by the differences between the LA and TA phonon branches and is considered in Sec. V.

At high temperatures $\Theta_D(T)$ can be expanded as a power series of $1/T^2$. This series is expected to converge rapidly at $T \gtrsim \frac{1}{2}\Theta_D$ and it is[27]:

$$\Theta_D^2(T)=\Theta_D^2(\infty)[1-A[\Theta_D(\infty)/T]^2+B[\Theta_D(\infty)/T]^4-\cdots]. \tag{2}$$

From this expansion, the values of $\Theta_D(\infty)$ for the various cuprous halides are extrapolated and they are given in Table I. In case both positive and negative ions are in the same effective field, $\Theta_D^2(\infty)$ is inversely proportional to the reduced mass[27] M:

$$\Theta_D^2(\infty) \propto M^{-1} = (m_1+m_2)/2m_1m_2. \tag{3}$$

For the three compounds the value of $\Theta_D(\infty)/M^{-1/2}$ is nearly constant at 1.87 and it appears as if the change in $\Theta_D/\Theta_D(\infty)$ for the various halides can be largely ascribed to the change in mass ratio. In Fig. 7 we plot the reduced $\Theta_D(T)/\Theta_D(\infty)$ against a reduced $T/\Theta_D(\infty)$ for the three halides, and this enables us to relate the plots directly to the mass changes of the halogen. The relative changes in the curve are: (a) $\Theta_D/\Theta_D(\infty)$ increases with the halogenic mass over all the range. This increase becomes more pronounced at $T \to 0$, near the minima and for $T/\Theta_D(\infty) \to \infty$. (b) the minimum in $\Theta_D/\Theta_D(\infty)$ shifts slightly to higher values of $T/\Theta_D(\infty)$.

The considerable drop in Θ_D observed in all cases at $T > 100$ °K (Figs. 4–6) cannot be explained by thermal expansion only and it must be attributed to the anharmonicity of the lattice vibrations, which is expected to become progressively more important as the amplitude of the vibrations increases. This anharmonicity tends to be the highest for CuCl. To illustrate this, we calculate the ratio of A/R_0, where A is the mean vibrational amplitude and R_0 is the interatomic distance at $T = 0$ °K, by a very simple model,[27] assuming that each ion is in the same field of force. We obtain

$$A/R_0 = \lambda[T/\Theta_D(\infty)]^2, \tag{4}$$

where

$$\lambda = \hbar[10/3MR_0^2k_B\Theta_D(\infty)]^{1/2}. \tag{5}$$

λ and R_0 are tabulated in Table I. λ may provide for an estimate of anharmonicity, and it is the largest for CuCl.

IV. LATTICE DYNAMICS

The lattice dynamics of ionic crystals can be adequately represented by the simple shell model introduced by Cowley *et al.*[30] The basic equation of this model is given by

$$\underline{M}_D\nu^2(\vec{q})\vec{u}(\vec{q}) = \underline{D}(\vec{q})\vec{u}(\vec{q}), \tag{6}$$

where $\underline{M}_D$ is a diagonal matrix representing the different atomic masses, $\vec{u}(\vec{q})$ is a column matrix representing the ionic polarization vectors, $\nu(\vec{q})$ are the eigenfrequencies, and $\underline{D}(\vec{q})$ is the dynamical matrix. All the matrices are of the order 6×6 and are functions of $\vec{q}$, the reduced wave-

TABLE I. All temperatures are given in °K. f_i is the ionicity defined by Phillips (Ref. 1). $\Theta_D(0)$, $\Theta_D(\infty)$ are the values extrapolated to 0 °K and to high temperature range. $\Theta_D^{\min}$ is the minimum measured value of the Debye temperature, M is the reduced atomic mass, and R_0 is the nearest interatomic distance. $\Theta_D^{el}(0)$ and λ are defined in the text.

Compound	f_i	$\Theta_D(0)$	$\Theta_D(\infty)$	$\Theta_D^{el}(0)$	$\Theta_D^{\min}$	$(M)^{-1/2}$	R_0(Å)	$10^2\lambda$
CuCl	0.746	164 ± 4°	280 ± 2°	180°	123°	0.148	2.34	4.85
CuBr	0.735	161 ± 2°	214 ± 1°	163°	121°	0.118	2.46	4.25
CuI	0.692	168 ± 1°	206 ± 1°	165°	130°	0.109	2.61	3.76

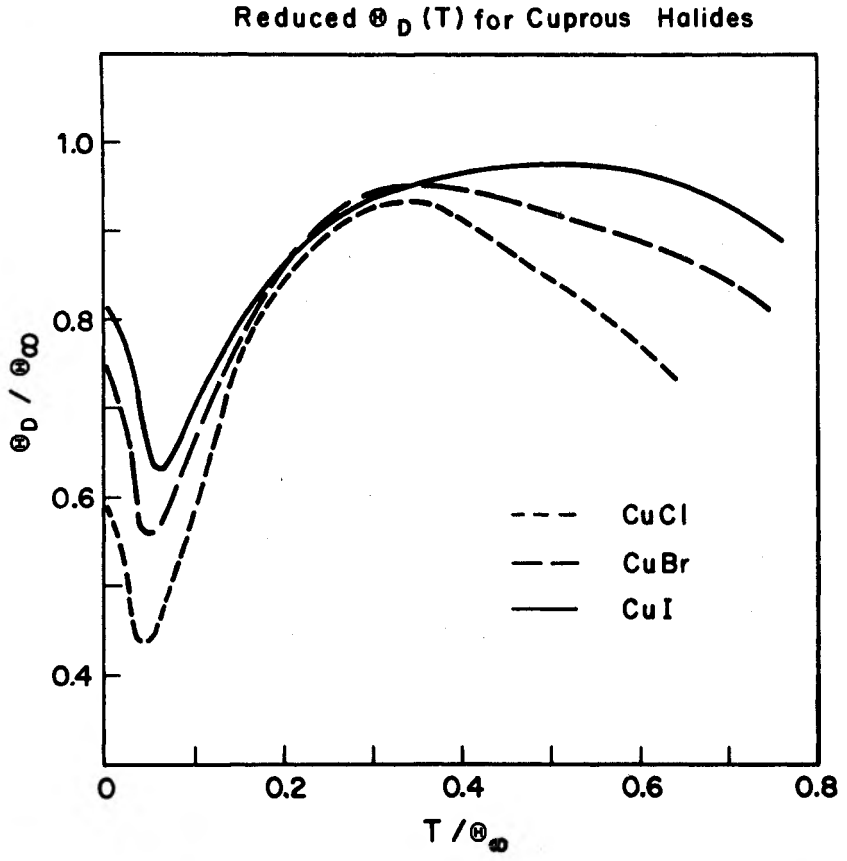

FIG. 7. Reduced plot of $\Theta_D/\Theta_D(\infty)$ against $T/\Theta_D(\infty)$ for the three cuprous halides.

number vector. $\underline{D}(\vec{q})$ is given by

$$\underline{D}(\vec{q})=\underline{R}(\vec{q})+\underline{Z}_D\underline{C}(\vec{q})\underline{Z}_D-[\underline{T}(\vec{q})+\underline{Z}_D\underline{C}(\vec{q})\underline{Y}_D]\times[\underline{S}(\vec{q})+\underline{K}_D+\underline{Y}_D\underline{C}(\vec{q})\underline{Y}_D]^{-1}[\underline{T}(\vec{q})+\underline{Y}_D\underline{C}(\vec{q})\underline{Z}_D], \tag{7}$$

where $\underline{Z}_D$, $\underline{Y}_D$, and $\underline{K}_D$ are all constant diagonal matrices. $\underline{Z}_D$ represents the ionic (core) charge numbers, $\underline{Y}_D$ gives the shells' charge numbers, and $\underline{K}_D$ represents the force constants between the shells and their inner cores. $\underline{C}(\vec{q})$ represents the long-range Coulomb interaction. The matrices $\underline{R}(\vec{q})$, $\underline{T}(\vec{q})$, and $\underline{S}(\vec{q})$ represent the various short-range interactions, namely, the core-core, core-shell, and shell-shell interactions.

The number of independent parameters for the short-range interactions is determined by the Zinc-blende (ZB) structure.[31] There are only two force constants, A and B, for the first neighbor (cation-anion) interaction. The second neighbor (anion-anion and cation-cation) interactions include at most eight possible force constants, which can be reduced to two only, namely, A'(Cu), $A''(X)(X=\mathrm{Cl,Br,I})$, by assuming central forces and by neglecting tangential forces, i.e.,

$$\left|\frac{\partial^2 v}{\partial r^2}\right| \gg \left|\frac{1}{r}\frac{\partial v}{\partial r}\right|.$$

Noncoulombic interactions of longer range are neglected.[24] For simplicity we also assume that the three matrices $\underline{R}$, $\underline{T}$, and $\underline{S}$ are equal,[30] which further reduces the number of short-range parameters to four only, namely, A, B, A'(Cu), and $A''(X)$.

Following the shell model,[30] we introduce shells for both ions $(\mathrm{Cu})^+$ and X^- with effective charges of ey(Cu) and $ey(X)$ and force constants K(Cu), $K(X)$ between every shell and its inner ionic core. Using all these assumptions, we have in total *nine* disposable parameters of which five are "electric" $[Z, Y(\mathrm{Cu}), Y(X), K(\mathrm{Cu}), K(X)]$ and four "repulsive" $[A, B, A'(\mathrm{Cu}), A''(X)]$.

Room-temperature dispersion relations $\nu_j(\vec{q})$ of the Cu halides where measured by inelastic coherent neutron scattering.[20-23] About 50 values of $\nu_j(\vec{q})$ were measured in each crystal along the major high-symmetry directions Δ [100], Σ [110], and Λ [111]. Using the above nine-parameter shell model, a least-squares fitting was performed, where the quality of fit is given by the criterion

$$P=\frac{1}{N-n}\sum_{i=1}^{N}\frac{[\nu_i(\mathrm{calc})-\nu_i(\mathrm{exp})]^2}{(\Delta\nu_i)^2}, \tag{8}$$

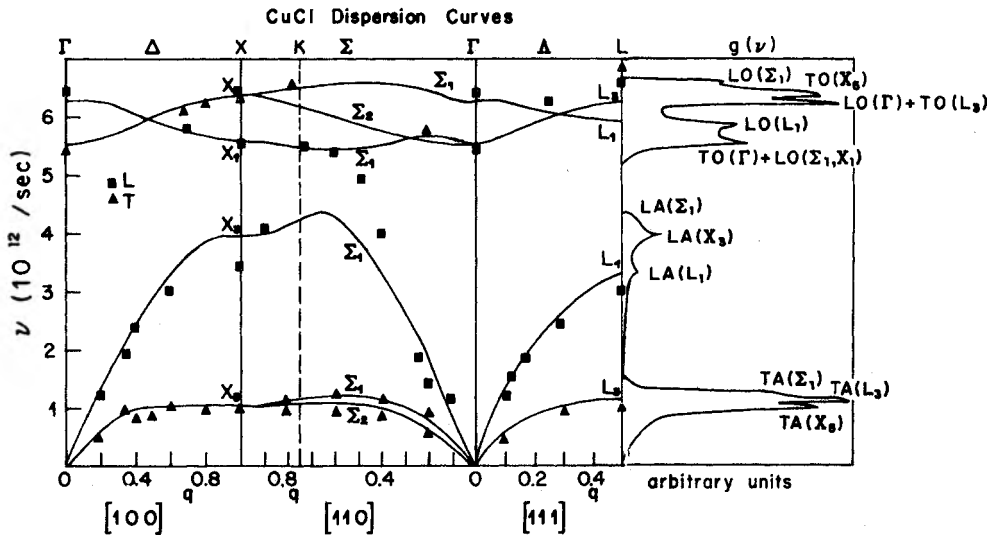

FIG. 8. Phonon dispersion relations of CuCl. The curves are derived from the nine-parameter shell model given in Table II. Experimental points are taken from Carabatos *et al.* (Ref. 20). $g(\nu)$ based on this model is shown as well.

where N is the number of the experimental frequencies, $n=9$ is the number of adjustable parameters of our model, ν_i(calc) and ν_i(exp) are the calculated and measured frequencies. $\Delta\nu_i$ is the experimental uncertainty in ν_i, taken here as $\Delta\nu_i/\nu_i = 0.05$ for most of the data points. A value of $P=1$ indicates a very good fit.

The fit to CuCl dispersion relations is shown in Fig. 8. The values of the adjusted parameters are given in Table II and $P=4.2$. The fit to the CuBr dispersion relation is of quality $P=1.4$ and it is shown in Fig. 9. The values of the best-fit parameters are also given in Table II. In this calculation the optical phonons were assigned only half the weight of the acoustical phonons because of the better accuracy of the latter. Our shell model yields a better fit with experiment with fewer parameters than the rigid-ion model of Prevot *et al.*,[21] who used 11 disposal parameters. Very recently Hoshino *et al.*[23] used a 14-parameter shell model to fit their 77 °K phonon dispersion relations, but their quality of fit is lower than ours. The fit to CuI phonon spectrum is shown in Fig. 10 and the parameters obtained are also given in Table II. The quality of fit is $P=1.2$. Our results give better fit to the measured TA branches along the Δ and Σ directions than the results of Hennion *et al.*[22] It should be mentioned, however, that in contrast to the case of CuCl, the phonon spectra of CuBr and CuI are very smooth and therefore considerably easier to be fitted by a force model. The sets of the shell-model parameters for CuBr and CuI given in Table II are not sensitive to small changes in the values of the individual parameters, so that slightly different models give almost as good fits as the best-fit values.

Our motivation for choosing the same nine-parameter shell model for the three crystals is that it enables us to draw comparisons between the various crystals in a systematic manner. We find that on going from CuI→CuBr→CuCl, that (a) the effective charge Z increases in accord with the ionicity of the compound, (b) The polarizability α of the halogen ion, estimated by $\alpha = e^2y^2/K$, increases while the polarizability of Cu^+ decreases at the same time. (c) The value of Cu-Cu short-range force constant A(Cu) increases in accord

TABLE II. Best-fit parameters of the shell model used to calculate $\nu_j(\vec{q})$ for CuX. The parameters are given in units of $e^2/2V_0$, where V_0 is the unit-cell volume. X represents Cl, Br, and I.

Crystal	Z	Y(Cu)	K(Cu)	$Y(X)$	$K(X)$	A	B	A'(Cu)	$A''(X)$
CuCl	0.33	−1.3	73.3	−2.2	24.0	9.3	8.4	4.0	−2.8
CuBr	0.30	−1.8	49.6	−0.7	87.9	5.7	6.7	1.0	2.1
CuI	0.29	−2.9	79.4	−0.3	85.9	9.9	10.3	0.6	3.1

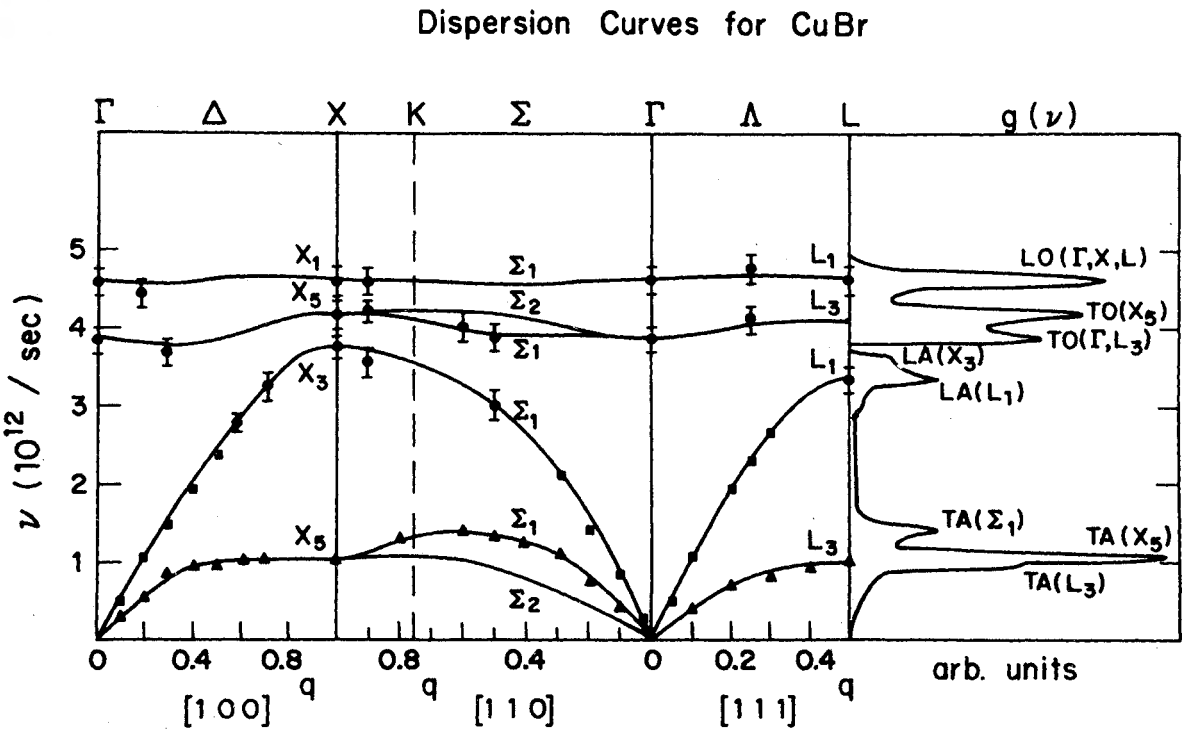

FIG. 9. Phonon dispersion relations for CuBr. The curves are derived from the nine-parameter shell model given in Table II. Experimental points are taken from Prevot *et al*. (Ref. 21). $g(\nu)$ based on this model is shown as well.

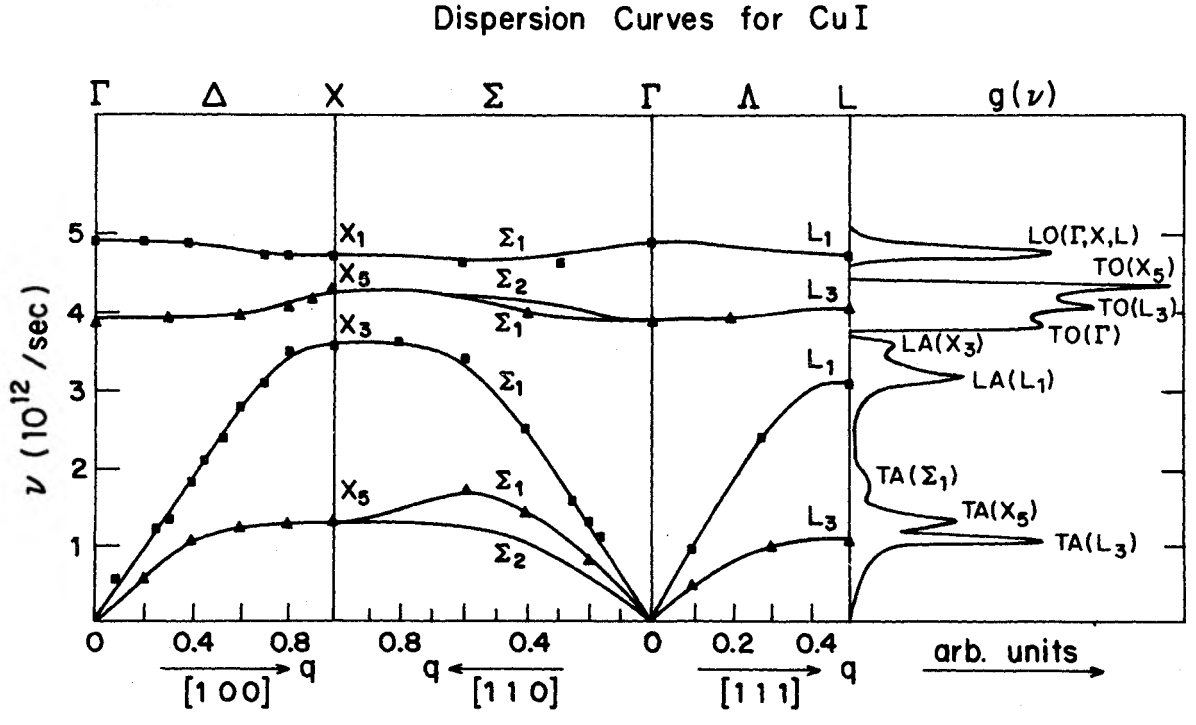

FIG. 10. Phonon dispersion relations for CuI. The curves are obtained from the nine-parameter shell model given in Table II. Experimental points are taken from Hennion *et al*. (Ref. 22). $g(\nu)$ based on this model is shown as well.

with the decrease in the interatomic distance.

Our findings may support the assumption that a possible interaction between the d electrons of neighboring Cu^+ ions would be most significant in CuCl. It is also interesting to note that in CuCl the force constant $K(Cl)$ that attaches the Cl^- shell to its inner core is very small, and that the Cl-Cl force constant $A''(Cl)$ is negative.

Of the three Cu halides the fit for CuCl by a simple shell model is the poorest. There exist more elaborate models that give better fits to the CuCl phonon spectrum,[24] and these are a "breathing" shell model and a "double" shell model.[24] However, the simple shell model is found adequate for our present purpose of treating the data of C_v.

V. COMPARISON BETWEEN EXPERIMENT AND THEORY

The shell-model parameters given in Table II, were used to calculate $\nu_j(q)$ as well as $g(\nu)$ for the three compounds. The results are shown in Figs. 8–10. In these calculations the extrapolation method[33] was used with 2992 crude mesh cubes uniformly distributed over $\frac{1}{24}$ of the first Brillouin zone. Two gaps are seen in each of the different $g(\nu)$. One is located between the optical and the acoustical modes and it becomes narrower on going from CuCl to CuI. The second gap is actually a low-density region appearing in the energy range of 2–3 THz, and it originates in the energy differences between the low-energy TA modes and the much higher LA modes. We believe that this gap is responsible for the large variation in the $\Theta_D(T)$ of the Cu halides. For CuCl $\Theta_D(T)$ varies between $\Theta_D(10\ ^\circ\mathrm{K}) = 120\ ^\circ\mathrm{K}$ and $\Theta_D(\infty) = 280\ ^\circ\mathrm{K}$.

The phonon densities of states were used to calculate the specific heats $C_v(T)$, using the following expression[36]:

$$C_v(T) = \frac{6Nh^2}{k_B T^2} \int_0^{\nu_{\max}} \frac{\nu^2 \exp(h\nu/k_B T)}{[\exp(h\nu/k_B T) - 1]^2} g(\nu)\, d\nu. \qquad (9)$$

A comparison between the calculated and measured $C_v(T)$ for the various crystals is shown in Figs. 1–3. There is an apparent agreement between theory and experiment where the average discrepancies between them are of about 2%. For CuCl the discrepancy increases above 90 °K and it is 5% at 155 °K. The reason for this may be due to anharmonic effects neglected in the theory.

A more sensitive comparison between theory and experiment is shown in Figs. 4–6. For CuCl, there is an excellent agreement between the calculated and measured $\Theta_D(T)$. Moreover, the extrapolated theoretical value of $\Theta_D(0) = 178\ ^\circ\mathrm{K}$ is in excellent agreement with the value of $\Theta_D(0^\circ) = 179.3 \pm 0.6$ extrapolated from measurements by Barron *et al.*[10] However, this excellent agreement is a little worrying, since the calculated $\Theta_D(T)$ is derived from a model that fits phonon dispersion relations at 300 °K, and is thus expected to be somewhat lower than the measured $\Theta_D(T)$. It is therefore suspected that this agreement is at least partly coincidental. To verify this, a second calculation, based on a double shell model (DSM)[24] was performed. The DSM gives a much better fit to the phonon dispersion relations of CuCl at 300 °K. Indeed, $\Theta_D(T)$ calculated from the DSM does not fit so well the observed $\Theta_D(T)$ below 30 °K, and it predicts $\Theta_D(0) = 146\ ^\circ\mathrm{K}$, much below the observed value of 179 °K.

In the cases of CuBr and CuI the fit between theory and experiment is very good in the range $15 < T < 95\ ^\circ\mathrm{K}$. The disagreements below 15 °K are to be expected for the same reason, (i.e., that the models are fitted to 300 °K phonon dispersion relations). In the higher range $T > 95\ ^\circ\mathrm{K}$, disagreements are to be anticipated because of anharmonicity that is not included in the theory. However, the disagreements in this range for CuI and CuBr are less pronounced than for CuCl. This shows, perhaps, that CuBr and CuI are less anharmonic than CuCl.

VI. GRÜNEISEN PARAMETER FOR CuCl

The Grüneisen parameter γ is defined within the quasiharmonic approximation by the following expression[32]:

$$\gamma = -\left(\frac{\partial \ln T}{\partial \ln V}\right)_s, \qquad (10)$$

or as a function of Θ_D derivatives

$$\gamma = -\frac{d \ln \Theta_D}{d \ln V}, \qquad (11)$$

where γ is a function of T. Another expression for γ is[32]

$$\gamma(T) = B_s V_m \beta / C_p, \qquad (12)$$

where V_m is the molar volume, B_s the adiabatic bulk modulus, and β the volume thermal-expansion coefficient.

Very recently, $\beta(T)$ for CuCl was measured by Barron *et al.*[10] in the range of 2–85 °K. They also measured C_p of CuCl in the range 2–16 °K and thus they were able to obtain $\gamma(T)$ for this range. Since our $C_p(T)$ measurements extends over a wider range of T, we use it here to obtain $\gamma(T)$ over the range $5 < T < 160^\circ$, where we use the data[9] for $\beta(T)$ and $V_m(T)$ above 85 °K. As for B_s, the values of[8,10] 0.44 Mbar below 30 °K and 0.43 above 30 °K are used. We also take $V_m = 23.8\ \mathrm{cm}^3$ at $T = 0\ ^\circ\mathrm{K}$ and $V_m(100^\circ) = 23.7\ \mathrm{cm}^3$.

The T dependence of γ is shown in Fig. 11. The

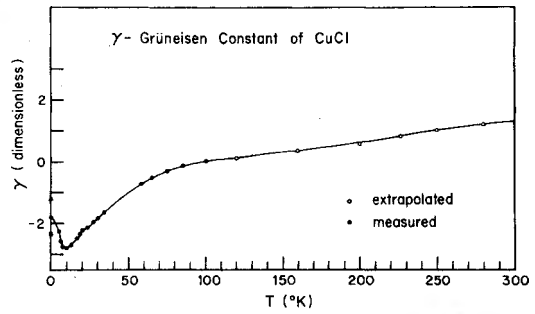

FIG. 11. Temperature dependence of the Grüneisen parameter γ for CuCl. The calculation is explained in the text. For $T < 95°$ we use the data of Barron *et al.* (Ref. 10) for β (marked as closed circles), for $T > 95$ °K the data of Shaake (Ref. 9) is used (marked as open circles). At $T = 0$, the values of γ_0 of Hanson *et al.* (triangle) (Ref. 8) and of Barron *et al.* (square) (Ref. 10) are shown as well.

value of $\gamma_0^{el} = -1.17$ shown separately in this figure was calculated[8,10] from elastic constants and it includes the piezoelectric effect. Our own value is $\gamma_0 = -1.86$. The marked disagreement between γ_0^{el} and γ_0 indicates that the true volume derivatives at low T differ considerably from the room-temperature values upon which the γ_0^{el} calculation was based. For comparison we also marked in Fig. 11 the limiting low T value $\gamma_0 = -2.4$ obtained by Barron *et al.*,[10] a value perhaps too low for CuCl.

The general behavior of $\gamma(T)$ looks normal when compared to other crystals such as Si, Ge, GaAs, InSb, CdTe, having similar structure.[11] In all these crystals $\gamma(T)$, as well as $\Theta_D(T)$, have a deep minimum at $T = \frac{1}{15}\Theta_D(0)$. At 300 °K, γ of CuCl is estimated to be 0.78.

The $\beta(T)$ data[9] for CuBr and CuI are presently inadequate to yield $\gamma(T)$ in detail. From existing data[9] we may expect $\gamma < 0$ for CuBr, while $\gamma > 0$ for CuI even at very low T. Negative γ is associated with negative thermal expansion, a phenomenon that is fairly common among covalent crystals possessing the Z.B. structure. It is interesting to note, however, that this effect is observed to increase with ionicity. Smith *et al.*[11] related γ_{min} and γ with ionicity for several Z.B. structure crystals and predicted the value of γ of AgI, CuCl, and CuBr to be the most negative among all these crystals.

The negative values of γ and β at low T may be related to the mode Grüneisen parameters[32] γ_j defined by

$$\gamma_j(\vec{q}) = -\frac{\partial \ln \nu_j(\vec{q})}{\partial \ln V} \tag{13}$$

in the quasiharmonic approximation. In terms of $\nu_j(\vec{q})$, the macroscopic γ is given by

$$\gamma = \sum_j \gamma_j C_j \Big/ \sum_j C_j, \tag{14}$$

where C_j is the Einstein specific-heat value that corresponds to ν_j. In this manner, the main contribution to γ at low T comes from low-frequency phonon branches (i.e., the TA modes) which are very flat in the Z.B. structure crystals. Force constants contribution to TA branches are largely tangential [i.e., they have the form $(1/r)\phi'(r)$] in contrast to radial forces of the type $\phi''(r)$ which contribute more to LA modes. Radial forces are expected to contribute positively to the individual γ_j while tangential forces contribute negatively.[32] It is therefore deduced that the mode Grüneisen parameter γ_j of the TA branches tends to bring down the value of $\gamma(T)$ at low T, an effect that is observed to increase with ionicity.[11] Among the Cu halides the largest negative Grüneisen parameter is observed for CuCl at low temperatures. Incidentally, AgI has the highest ionicity[1] ($f_i = 0.770$) among all Z.B. structure crystals and its β and γ values are negative even at room temperature.[34] On the other hand, CuI has positive γ_0 despite its high ionicity.[9]

The reason that CuI has positive γ_0 is related to the relative volumes of the ions forming the crystal. The Z.B. structure, which is usually quite open, consists of two interpenetrating fcc sublattices. If we compare the ionic radii R_X of the various halides[35] ($R_{Cl} = 1.81$ Å, $R_{Br} = 1.96$ Å, $R_I = 2.20$ Å) with the nearest halide-halide distance R_0', given by $\sqrt{\frac{8}{3}}R_0$ where R_0 is listed in Table I, we observe that at $T = 0$ °K for CuCl and CuBr $R_0' > 2R_X$, while for CuI, $R_0' < 2R_I$. This means that in the cases of CuCl and CuBr the distance between the two halides is larger than the sum of their radii, and this permits negative β and γ. In contrast, for CuI the iodine-iodine distance is smaller than twice the iodine radius and this allows only for positive β and γ.

VII. CONCLUSION

The specific heat C_p of the cuprous halides CuCl, CuBr, and CuI was measured in the temperature range of 5 to 160 °K. It was also expressed in terms of $\Theta_D(T)$ and considerable variations in $\Theta_D(T)$ were found over this range. The largest variations were for CuCl and less so for CuBr and CuI. These variations are partly related to the gap in $g(\nu)$ caused by the energy differences between the TA and the LA modes. This gap is large for CuCl and becomes smaller forCuBr and CuI. For higher temperature range the $\Theta_D(T)$ curves tend to bend downwards due to anharmonic effects. This tendency is more accentuated for CuCl and less so for CuBr and CuI.

In order to correlate the specific-heat data with more detailed information of the phonon spectra derived from inelastic-neutron-scattering data, a nine-parameter simple shell model was applied to fit the observed phonon dispersion relations of the three Cu halides. The quality of fit of this model for CuBr and CuI to the slow neutron scattering data was at least as good as that accomplished by shell models employing more parameters.[21-23] In the case of CuCl, the success of this model was considerably less although it was adequate for the purpose of correlating the specific-heat data to the observed phonon dispersion relations. The motivation for using the same model for the different halides was to look for general trends in behavior. It was found that the nearest Cu-Cu forces were attractive and tended to decrease on going from CuCl to CuI. The Cu-Cu forces are probably related to the strong anharmonicity in CuCl and CuBr as well as to the negative thermal expansion at low T observed in these crystals. The fit of the models to the measured $\Theta_D(T)$ was good for $T > 30$ °K. Below 30 °K, the fit was less good and this is expected since the phonon data were measured at room temperature.

In the case of CuCl, the Grüneisen parameter $\gamma(T)$ was calculated in the range of 5 to 160 °K. There is a discrepancy between the measured γ_0 and γ_0^{el} calculated from the elastic constant data of CuCl. In the case of CuI, γ_0 is positive in contrast to CuBr and CuCl and this is simply explained by atomic volume considerations that indicate that iodine ions form a closed structure in the case of CuI.

ACKNOWLEDGMENTS

We wish to thank Professor J. Makovsky for supplying us the ingot of CuI used for the measurements, and Dr. I. Kaminow from the Bell Telephone Laboratory, for supplying us a single crystal of CuBr. We also wish to express gratitude to Dr. A. Pasternak for his help in programming, and Drs. T. H. K. Barron, J. A. Birch, and G. K. White for their unpublished thermal data of CuCl at low temperature.

---

*In partial fulfillment of the D.Sc. thesis at the Physics Department of the Technion-Israel Institute of Technology, Haifa, Israel.

†Present address: Physics Department, University of Toronto, Ontario, Canada.

[1]J. C. Phillips, Rev. Mod. Phys. 42, 317 (1970).
[2]J. A. van Vechten, Phys. Rev. 182, 891 (1969).
[3]E. Rapaport and C. W. F. T. Pistorious, Phys. Rev. 172, 838 (1968).
[4]O. Brafman, M. Cardona, and Z. Vardeny, Phys. Rev. B 15, 108 (1977).
[5]V. Meisalo and M. Kalliomäki, High Temp.-High Pressure 5, 663 (1973).
[6]C. W. Chu, S. Early, T. M. Geballe, A. Rusakov, and R. E. Schwall, J. Phys. C 8, 1241 (1975).
[7]R. C. Hanson, J. R. Halberg, and C. Schwab, Appl. Phys. Lett. 21, 490 (1972).
[8]R. C. Hanson, K. Helliwell, and C. Schwab, Phys. Rev. B 9, 2649 (1974).
[9]H. P. Schaake, AFCRL Report No. 69-0538, quoted by N. Plendle and L. C. Mansur in Appl. Opt. 11, 1194 (1972).
[10]T. H. K. Barron, J. A. Birch, and G. K. White, J. Phys. C 10, 1617 (1977).
[11]T. F. Smith and G. K. White, J. Phys. C 8, 2031 (1975).
[12]T. Fukumoto, S. Nakashima, K. Tabuchi, and A. Mitsuiski, Phys. Status Solidi B 73, 341 (1976).
[13]J. E. Potts, R. C. Hanson, C. T. Walker, and C. Schwab, Phys. Rev. B 9, 2711 (1974).
[14]I. P. Kaminow and E. H. Turner, Phys. Rev. B 5, 1564 (1972).
[15]M. Krauzman, P. M. Pick, M. Paulet, G. Hamel, and B. Prevot, Phys. Rev. Lett. 33, 528 (1974).
[16]A. Hadni, F. Brekat, J. Claudel, and P. Strimer, J. Chem. Phys. 49, 471 (1968).
[17]M. Ikezawa, J. Phys. Soc. Jpn. 35, 309 (1973).
[18]J. Ruvalds and A. Zawadowski, Phys. Rev. B 2, 1172 (1970); Solid State Commun. 9, 129 (1971).
[19]B. Dorner, B. Hennion, B. Prevot, and R. M. Pick, Report. No. 0402019 Saclay Laboratoire de Spectroscopie, L.A. 232 CNRS-Strasbourg (unpublished).
[20]C. Carabatos, B. Hennion, K. Kunc, F. Moussa, and C. Schwab, Phys. Rev. Lett. 26, 770 (1971).
[21]B. Prevot, C. Carabatos, and C. Schwab, Solid State Commun. 13, 1725 (1973).
[22]B. Hennion, F. Moussa, B. Prevot, C. Carabatos, and C. Schwab, Phys. Rev. Lett. 28, 964 (1972).
[23]S. Hoshino, Y. Fujii, J. Harada, and J. D. Axe, J. Phys. Soc. Jpn. 41, 965 (1976).
[24]Z. Vardeny, G. Gilat, and A. Pasternak, Phys. Rev. B 11, 5175 (1975).
[25]Z. Vardeny, D. Moses, G. Gilat, and H. Shechter, Solid State Commun. 18, 1369 (1976).
[26]J. de Launay, Solid State Phys. 2, 219 (1956).
[27]T. H. K. Barron, W. T. Berg, and J. A. Morrison, Proc. R. Soc. A 242, 478 (1957).
[28]A full description of the calorimetric system will be published elsewhere.
[29]G. T. Furukawa, W. G. Saba, and M. L. Reilly, Handb. Chem. Phys. 55, D-72 (1974).
[30]R. A. Cowley, W. Cochran, B. N. Brockhouse, and A. D. B. Woods, Phys. Rev. 131, 1026 (1962).
[31]F. Herman, J. Phys. Chem. Solids 8, 405 (1959).
[32]T. H. K. Barron, J. Appl. Phys. 41, 5044 (1970).
[33]G. Gilat and L. J. Raubenheimer, Phys. Rev. 144, 390 (1966).
[34]S. Hoshino, J. Phys. Soc. Jpn. 12, 315 (1957).
[35]*Handbook of Chemistry and Physics*, 55th ed. PF198 (Chemical Rubber, Cleveland, 1975).
[36]C. Kittel, *Introduction to Solid State Physics*, 4th edition (Wiley, New York, 1971), pp. 210-217.